Study of the Interaction of Segmental Peptides of α-Synuclein with Phospholipid by Langmuir Monolayer and Surface FT-IR Technique

by

Christopher Ewuola

A Thesis Presented to the

Graduate Faculty of Middle Tennessee State University

In Partial Fulfillment of the Requirements

for the Degree Master of Science

October, 2022

Acknowledgment

I would like to thank my research advisor Dr. Chengshan Wang for his unending support and guidance in completing my research. He stood by me in the most difficult time and was always available when I needed clarifications even on weekends when he should be resting. Indeed, I would not have made the progress I made in my research if not for his selflessness. I will also love to thank Dr. Andrienne C. Friedli for her advice in choosing my coursework intentionally in a bid to free up time to work on my thesis research and thesis writing at the tail end of my program. I want to thank my committee members Dr. Charles C. Chusuei and Dr. Keying Ding for taking time out of their busy schedules to read my thesis and for their input, guidance, and corrections on my thesis.

I would like to thank every member of the faculty for making my stay at MTSU a memorable one and for the understanding they showed when I had to use some of the analytical instruments for a long stretch of time. I would also like to thank Mr. Jessie Weatherly for being there to help any time I am having trouble with any of the instruments, especially the FTIR. I also want to thank members of my research team both past and present for their guidance and help with the necessary information I needed.

Lastly, I would also like to thank my family for always being there through it all, their encouragement and prayers saw me through my master's program.

ABSTRACT

Study of the Interaction of Segmental Peptides of α-Synuclein with Phospholipid by Langmuir Monolayer and Surface FT-IR Technique

Ewuola Christopher

α-Synuclein (α-syn), which is a protein contains 140 amino acid residues, is the major protein component of Lewy bodies, the hall mark deposition of Parkinson's disease (PD).1 Segment peptides of α-syn was also detected in Lewy bodies together with phospholipids. Despite the abundance (~ 1 % among the total proteins) in the brain, α-syn accumulates in the presynaptic terminals where exists high concentration of amphiphilic structure (e.g., liposomes and cell membrane) comprising phospholipids.2 Therefore, it is important to study the interaction between α-syn segmental peptides and phospholipids. Previously, α-syn has been spread at the air-water interface by Langmuir monolayer technique which was used to mimic the amphiphilic nature in vivo.3 Spectroscopic and surface FTIR results showed that α-syn transformed from unstructured conformation in aqueous solution to α-helix at the interface in a monolayer structure. Here, the interaction of phospholipid with several segmental peptides of α-syn by spreading phospholipid at the interface to form monolayer in the presence of several segmental peptides of α-syn. From surface FTIR results, the tilted angle of the alkyl chain in the pure phospholipid monolayer is 79°±1°. Among segmental peptides, three longer peptides (i.e., α-syn(66-85), α-syn(61-95), and α-syn(57-102)), which can form Langmuir monolayer by themselves, were found not to interact substantially with phospholipid because the titled angle of alkyl chain of phospholipids keeps at 79°±1°. Differently, a shorter segmental peptide α-syn(71-82) interacts with phospholipids intensively and changes the tilted angle of alkyl chain of phospholipid to 76°±1°.

TABLE OF CONTENTS

LIST OF FIGURES

LIST OF TABLES

SCHEMES

Chapter 1 Introduction

1.1 Structural Biology

Proteins are complex biological macromolecules, consisting of chains of amino acids covalently linked by amide bonds. All the proteins found in biological systems are composed of 20 different amino acids. Amino acid consists of amino group, carboxylic acid group, and an α-carbon which links R groups to the amino acid. Figure 1-1 shows the structure of an amino acid where R group is also called residue group and amino acids are distinguished based on the structure of R group (Table 1).[1]

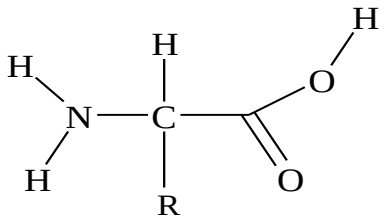

Figure 1.1 Structure of an amino acid

Table 1. Structure of R group of different amino acids

Amino acid	**Abbrevations**		**Structure of R group**
Alanine	Ala	A	$-CH_3$
Arginine	Arg	R	$-(CH_2)_3-NH-C(NH_2)=NH$
Asparagine	Asn	N	$-CH_2-CO-NH_2$
Aspartic acid	Asp	D	$-CH_2-COOH$
Cysteine	Cys	C	$-CH_2-SH$

Glutamine	Gln	Q	$-(CH_2)_2-CO-NH_2$
Glutamic Acid	Glu	E	$-(CH_2)_2-COOH$
Glycine	GlY	G	-H
Histidine	His	H	$-CH_2C_3H_3N_2$
Isoleucine	Ile	I	$-CH(CH_3)-CH_2-CH_3$
Leucine	Leu	L	$-CH_2-CH-(CH_3)_2$
Lysine	Lys	K	$-(CH_2)_4NH_2$
Methionine	Met	M	$-(CH_2)_2-S-CH_3$
Phenylalanine	Phe	F	$-CH_2-C_6H_5$
Proline	Pro	P	$-CH(CH_2)_3NH$
Serine	Ser	S	$-CH_2-OH$
Threonine	Thr	T	$-CH(OH)-CH_3$
Tryptophan	Trp	W	$-CH_2-C_8H_6N$
Tyrosine	Tyr	Y	$-CH_2-C_6H_5-OH$
Valine	Val	V	$-CH-(CH_3)_2$

Essential to life processes, proteins perform a variety of functions, including catalyzing metabolic reactions, replicating DNA, responding to stimuli and so on.[2-5] On the other hand, the malfunction of proteins has been shown to be related to many diseases.[6-7] Therefore, the elucidation of proteins structure will not only helps to understand how proteins work in vivo but also provide pathological information about various diseases. As a consequence, structural biology which focuses on the elucidation of the proteins structure

has attracted extensive scientific attractions. Several levels of protein structure are discussed below.[8-12]

1.2 Protein Structure

1.2.1 Primary Structure

Amino acids are covalently linked together by amide bonds (i.e., CO-NH), formed between the amine group of one amino acid and the carboxyl group of the adjacent amino acid. A chain of amino acids connected by amide bonds is referred to as a polypeptide chain. The two termini of a polypeptide chain are called N-terminus (it has free amine group) and C-terminus (it has free carboxylic acid group). Polypeptide is usually written from N-terminus end to C-terminus end.[6-8] Scheme 1.1 the primary structure of α-synuclein which will be extensively discuss below.[13-14]

MDVFMKGLSK AKEGVVAAAE KTKQGVAEAA GKTKEGVLYV GSKTKEGVVH GVATVAEKTK EQVTNVGGAV VTGVTAVAQK TVEGAGSIAA ATGFV*KKDQL GKNEEGAPQE GILEDMPVDP DNEAYEMPSE EGYQDYEPEA*

Scheme 1.1 The sequence of α-synuclein with the N-terminus underlined and the C-terminus expressed in Italics.

1.2.2 Secondary Structure

Proteins/peptides can fold to form secondary structure by the intra and intermolecular hydrogen bonds among the amino acid residues. Common secondary structures (also called

as conformations) are α-helix, β-sheets, and random coils as shown in Figure 1.2.[6-8] Random coils structure is also called unstructured conformation, in which the polypeptide chain is well distributed in the aqueous solution and moves freely in the aqueous environment. The α-helical structure looks like a spring as shown in Figure 1.2. α-Helix is characterized by the intra molecular hydrogen bonds between the amino group of one amino acid and the carbonyl group of other amino acid located 3~4 residues away along the polypeptide chain. These hydrogen bonds are usually present parallel to the helical axis. The α-helix is usually right-handed and contains approximately 3.6 amino acid residues per turn. Formation of hydrogen bonds create helical structure of polypeptide chain, as a result side chains of amino acids protrude from outside of helix.[6-8]

The structural units of β-sheets are strands also shown in Figure 1.2. It is a fully extended structure characterized by multiple strands (polypeptide chains) arranged side-by-side. Each β-sheet contains 6 to 22 strands. Side chains are present above and below the plane of polypeptide chain. Inter-strain hydrogen bonds are formed between the carbonyl oxygen of one chain and the amide hydrogen of other chain. β-sheet sheets are of two types i.e. parallel and anti-parallel sheets. In a parallel sheet, two strands run in the same direction.i.e. from N-terminus to C-terminus. In an anti-parallel sheet, both the strands run in opposite direction, meaning if one strand runs from N- terminus to C-terminus, another strand runs from C-terminus- N-terminus.[6-8]

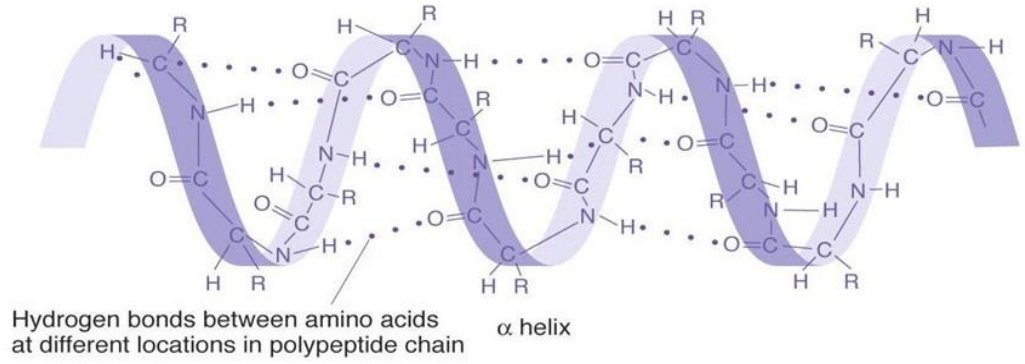

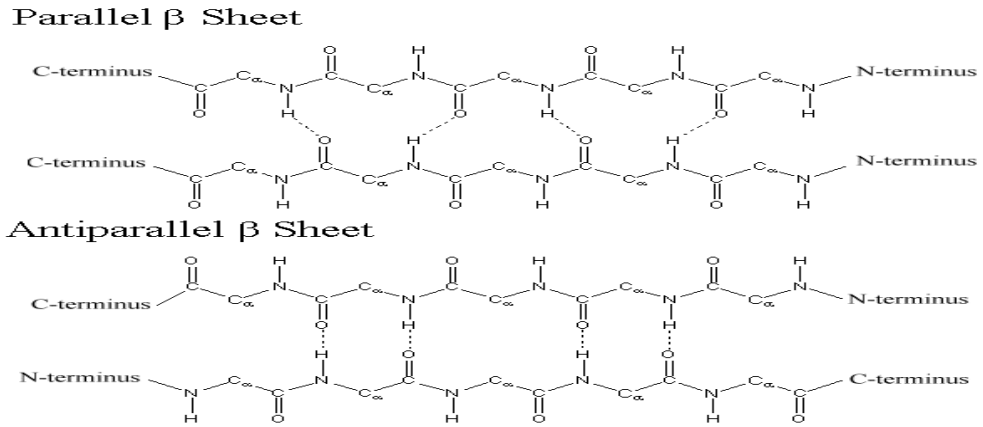

Figure 1.2. Illustration of secondary structures.

1.2.3 Tertiary and Quaternary Structure

Tertiary structure arises when secondary structure elements pack tightly to form the well-defined 3D structure termed as tertiary and quaternary structures. It is usually stabilized by four forces, hydrophobic forces, covalent bond, Vanderwall interaction, and hydrogen bonds. Among these four forces, hydrophobic interactions among the secondary structural elements play an important role in stabilizing the structure.[6-8] Among proteins,

α-synuclein shown in Scheme 1.1 can form various structure mentioned above and has attracted extensive scientific notations due to its involvement in Parkinson's disease (PD) as below.[13-14]

1.3 α-Synuclein and PD

Parkinson's disease (PD) is hallmarked by the abnormal aggregation of α-synuclein (α-syn) which is a 140-amino-acid protein with its sequence shown in Scheme 1.1 above.[15] The primary structure of α-syn (Scheme 1.1) constitutes three domains:[16] N-terminus (residues 1–60), the nonamyloid component (NAC) spanning residues 61–95, and C-terminus with residues 96–140.[16-17] Among the three domains, only the nonamyloid component (NAC) part (referred as α-syn(61-95) hereafter) is responsible for its aggregation.[16] In addition, considerable segmental peptides of α-syn have been detected in the lesion region in the PD patients brain.[18] Among the segment peptides, the NAC segment or α-syn(61-95) is an important one.[18] Especially, segment peptides have been detected to coaggregate with β-amyloid protein in the senile plaques in the brain of Alzheimer's disease (AD) patients.[19] To determine the structure of α-syn, various techniques have been used and the major methodology is below.

1.4 Techniques to clarify protein Structure

1.4.1 X-ray crystallography

X-ray crystallography is the most widely used method to address proteins structure and the detailed proteins structure can be determined in atomic level.[8, 20] Most of the proteins structures in protein data bank were determined by this method.[1] However, this technique has some drawbacks. First, proteins should be in single crystallized form and there is no particular common method of crystallization which can be applied to all proteins. Lots of proteins are difficult to form single crystal structure. For example, α-syn cannot form single crystal structure and no report has been published about its single crystal structure.

1.4.2 Nuclear Magnetic Resonance (NMR) Spectroscopy

Another powerful technique is multi-dimensional NMR technique which can also provide high resolution results for proteins.[3] Monomer α-syn is unstructured in aqueous solution and transforms to α-helix in the presence of phospholipids vesicles.[15, 21] Although hindered by the low tumbling rates of vesicles,[22-23] NMR still provided detailed structure of α-helical monomer α-syn with vesicles in high resolution, because the stability of α-helical monomer α-syn does not challenge the long time measurements of multi-dimensional NMR.[15, 21] As for the aggregates of α-syn (i.e., the hallmark of PD as mentioned above), two types of aggregates (i.e., mature fibrils and oligomers) has been reported.[15, 21] After long time measurements also due to the stability of mature fibrils, solid

state NMR showed that the NAC part of α-syn chain is in β-sheet conformation while the C-terminal residues still remained in unstructured conformation in mature fibrils.[24] Recently, the strand of the NAC part in the mature fibrils of α-syn was shown to be with an in-register structure.[25]

As compared to mature fibrils and α-helical monomer α-syn in the presence of vesicles, the structure of the oligomer of α-syn is very important for PD pathology. The oligomer can bind with the cell membrane to form pore structure, consequently causing the leakage of cytosol and destroying the homeostasis of the cellular species. Thus, the pore structure has been shown to be responsible for the loss of the neuronal cells.[17, 26-27] Therefore, elucidating the structure of the pore structure formed by the oligomer of α-syn is essential, not only for the PD pathology but also important for therapeutic agent development for PD. However, the information about the structure of the oligomer of α-syn with high resolution is limited. Unlike mature fibrils and α-helical monomeric α-syn in the presence of vesicles, oligomer of α-syn has been indicated to have a short life-time. This challenges NMR which usually needs long time measurement.[21] Therefore, other techniques with quick response were also employed.

1.4.3 Circular Dichroism (CD) Spectroscopy

Circular dichroism is a consequence of the interaction of polarized light with chiral molecules. Chiral molecules make up the vast majority of biological compounds. For instance, 19 of the 20 common amino acids that make up proteins are chiral. The primary use of circular dichroism analysis is the study of biological molecules because of the highly chiral chemistry of these molecules.

To truly grasp circular dichroism, one must first grasp the fundamentals of polarization. Linearly polarized light has oscillations that are contained inside a single plane. All polarized light states can be described as a sum of two linearly polarized states at right angles to each other, usually referenced to the viewer as vertically and horizontally polarized light. If for instance, we take horizontally and vertically polarized light waves of equal amplitude that are in phase with each other, the resultant light wave is linearly polarized at 45 degrees. If the two polarization states are out of phase, the resultant wave ceases to be linearly polarized. For example, if one of the polarized states is out of phase with the other by a quarter-wave(an optical element that converts between linearly polarized light and circularly polarized light), the resultant will be a helix and is known as circularly polarized light (CPL). The helices can be either right-handed (R-CPL) or left-handed (L-CPL) and are non-superimposable mirror images.[47]

There is a long history of CD studies about peptides and proteins in the biochemical and biophysical science. CD is very sensitive to protein conformation and is a fast method for monitoring structural changes in protein, because the measurement of CD can be accomplished in several minutes. Because of the large amount of carbonyls (C=O which absorbs intensively around 200 nm) in the amide bonds, proteins usually show strong CD signals between 260 and 180 nm. Since the carbonyls are arranged differently in conformations (such as α-helix, β-sheets, and unstructured conformation), every secondary structure shows its distinct patterns in CD spectrum as below.[28]

The Far UV-CD spectra of the α-helix conformation have two characteristically negative peaks at 222 and 209 nm and one positive peak at 192 nm. The Far UV-CD of β-

sheet conformation exhibits a positive peak at 196 nm and a negative peak at 215 nm. As for the unstructured conformation, only one negative peak at 199 nm will be detected. Similarly, every conformation can also show their distinct patterns in the FTIR spectroscopy.

1.4.4 FTIR Spectroscopy

FTIR spectroscopy is also an important technique to evaluate the major secondary structure in a peptide/protein. This is achieved by the characteristic peak position of amide I band (from 1600 to 1700 cm^{-1}), which mainly stems from the stretching mode vibration of the backbone carbonyls (i.e., C=O). For example, the amide I band of α-helix is around 1650 cm^{-1}, whereas that of β-sheet is at 1630 cm^{-1}, and that of the unstructured conformation is at 1640 cm^{-1}.[29] By deconvoluting the amide I band, the major conformation in a peptide/protein can be evaluated.[29-30] Together with supported phospholipids bilayer (SPB)structure mimicking cell membrane,[3, 31] surface FTIR techniques have been widely used to evaluate the orientation of membrane peptides/proteins at interface.[29, 32-33] Two major surface FTIR techniques, namely, Infrared Reflection Absorption Spectroscopy (IRRAS) and p-polarized Multiple Angle Incidence Resolution Spectroscopy (pMAIRS), are discussed in Scheme 1.2 below.[34-36]

1.4.5 Surface FT-IR Techniques

For both IRRAS and pMAIRS, the p-polarized IR beam is induced to irradiate on the surface of the substrate[34-36] and the incident angle of the IR beam (θ in Scheme 2) is

variable. For the p-polarized IR beam, the electronic field is in the plane of the IR beam with surface normal and perpendicular to the forward direction of the incident beam. The IRRAS detects the reflected IR beam (Scheme 2A) whereas pMAIRS detects the transmitted one (Scheme 2B). As for IRRAS which was developed earlier, p-polarized IR beam will not be reflected around the Magic Angle (or Brewster angle around 53.5 ° - the angle of incidence at which the reflected light is completely plane polarized). Therefore, although IRRAS has been used to evaluate the orientation of peptides/proteins at the interface,[34-35] quantitative measurement of the tilted angle of vibrations is difficult. As a recently developed technique, pMAIRS can be utilized on many more substrates than that of Attenuated Total Reflection (ATR).[37-38] In addition, the spectrum in-plane (i.e., S_{IP} in Scheme 2B) and spectrum out-of-plan (S_{OP} in Scheme 2B) can be obtained. The tilted angle of any vibration can be quantitatively determined by the ratio of the peak intensity in S_{IP} and S_{OP}.

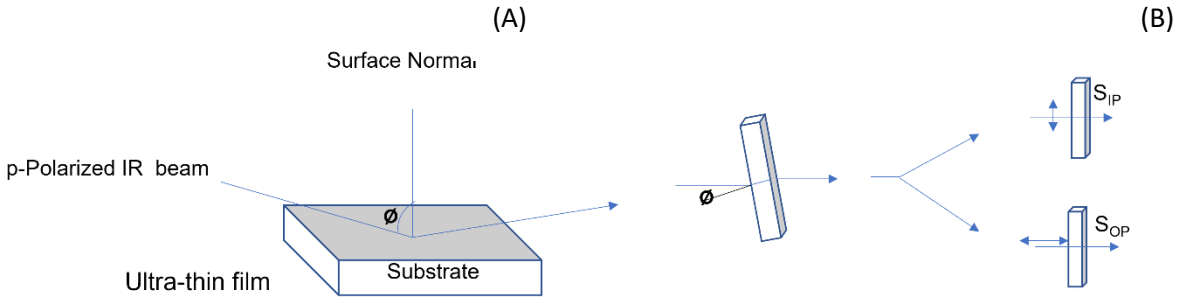

Scheme 1.2. Illustrations of (A) IRRAS and (B) pMAIRS with variable incident angle θ in both techniques.[37]

The tilted angle/orientation of various conformations or secondary structures can also be accurately determined as shown below in Scheme 1.3. As for α-helix, the vibration of the stretching mode of the backbone C=O is roughly parallel to the direction of the axis of α-helix as shown in Scheme 1.3.[39] Since the amide I band is mainly from the stretching mode of the backbone C=O, the orientation of the axis of α-helix can be determined by the amide I band in pMAIRS. Thus, our group has used pMAIRS to study α-syn and its segments.

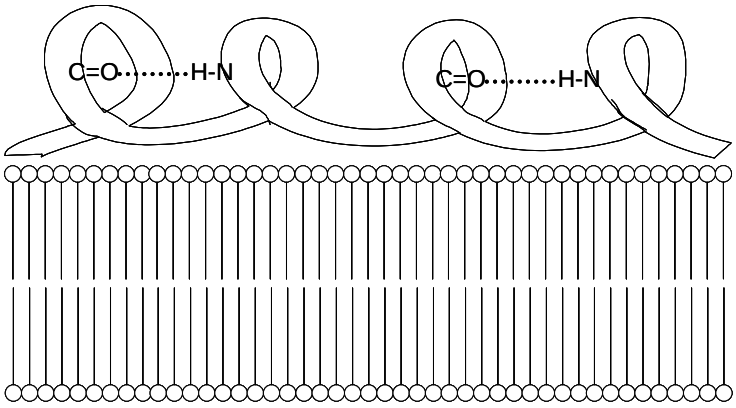

Scheme 1.3. The illustration about the orientation of α-helix on phospholipid bilayer

1.5 Efforts to Elucidate the Structure of α-Syn by IRRAS and pMAIRS

1.5.1 α-Syn and Langmuir monolayer Technique

As mentioned in Section **1.3**, α-syn is the hallmark protein of PD. Despite the abundance in the brain,[15-16] α-syn accumulates in the presynaptic terminals where the concentration of amphiphilic structure (e.g., liposomes and cell membrane) is high.[30, 40] Thus, the interaction of the amphiphilic structure with α-syn has attracted extensive scientific attentions.[41-43] On

the other hand, the reason of the accumulation of α-syn in the presynaptic terminals has been unclear because of the complication of the amphiphilic structure. The structure of a liposome or cell membrane (i.e., the above-mentioned amphiphilic nature) can be further divided into three detailed region as shown in Scheme 1.4:[44] (i)the interior core of the membrane, which has a hydrophobic character; (ii) the hydrophilic headgroups of the lipids; (iii) the lipid-water interfacial layer at which the dielectric constant is smaller than the bulk water of the cell matrix.[45-46]

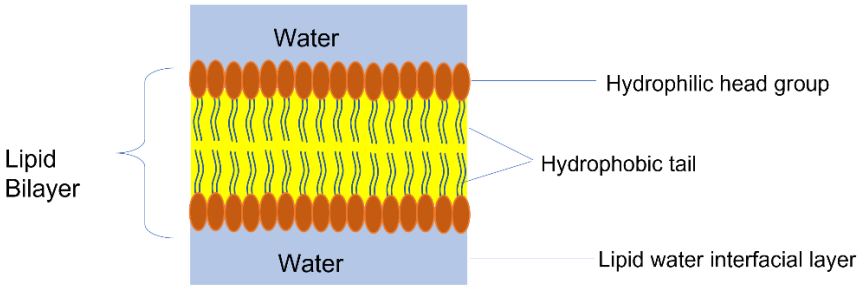

Scheme 1.4. Basic structure of lipid bilayer.

The properties of air-water interface has been found to be similar to those of the lipid-water interfacial layer.[38, 46] Furthermore, the accumulation and the interaction between the proteins/peptides molecules at the interface can be precisely monitored by a Langmuir monolayer technique.[38] In addition, the conformation of proteins/peptides at the interface can be also determined by CD and surface FT-IR mentioned above. Therefore, our research group has studied both the conformation and orientation of α-syn and its NAC part by Langmuir monolayer technique and surface spectroscopy as below.

1.5.2 α-Syn Transforms to α-Helix at Interface

The α-syn whole protein was first studied by Langmuir monolayer technique and α-syn has been shown to form a Langmuir monolayer at the air-water interface, and the monolayer was found to be stable.[24] As previously stated in Section 1.2, that α-synuclein in aqueous solution is in an unstructured conformation which has never been reported to form a stable Langmuir monolayer. Thus, it is very interesting to study the conformation of α-synuclein at the air-water interface. α-Helix is characterized by two negative peaks at 222 nm and 208 nm with one positive peak at 192 nm.[24] These peaks were observed when the CD spectrum of quartz slides was deposited with α-synuclein Langmuir monolayer. This is an indication that α-synuclein is in α-helix rather than unstructured conformation at the air-water interface. For further confirmation, the surface FTIR spectra of α-synuclein detected the Amide I band at 1655 cm^{-1}, which is assigned to α-helix. Therefore, by combining the results of Langmuir monolayer technique, CD, and FTIR, it can be concluded that the unstructured α-synuclein in aqueous solution transforms to α-helix when spread at the air-water interface. [24]

1.5.3 NAC Segment also Transforms to α-Helix at Interface

As an important segment of α-syn, our research group also synthesized NAC segment (termed as α-syn(61-95) hereafter) and studied its surface property. Similar to the whole protein, α-syn(61-95) is unstructured in aqueous solution and also forms a stable

Langmuir monolayer (indicated by surface pressure above 18mN/m) at the air-water interface.[38] In addition, α-syn(61-95) also transforms to α-helix according to both the CD and pMAIRS results. More importantly, pMAIRS measured the axis of the α-helical α-syn(61-95) at the interface to be 32.2 º, even in the monolayer at the interface.[38] As mentioned above, neither X-ray crystallography nor NMR can provide structural information for proteins/peptides in monolayer structure. Therefore, pMAIRS can supplement X-ray and NMR to address membrane proteins/peptides structure.

1.6 Thesis proposal

In addition to α-syn(61-95), other segment peptides of α-syn also attracted scientific notations. For example, α-syn(71-82) which spans residues 71 to 82 in the sequence of to α-syn was shown to be critical for the aggregation.[1] Furthermore, α-syn(61-95) is hydrophobic and α-syn(57-102) was reported to be more soluble in water as well as more similar to the whole protein of α-syn.[16] On the other hand, the air-water interface is more similar to the lipid-water interfacial layer. The effect of hydrophobic chain of phospholipid has not been studied yet. Hence this thesis is focused on the following:

1. To evaluate the effect of the hydrophobic and hydrophilic head groups of phospholipid bilayer in segmental peptides-lipid interaction
2. Use pMAIRS to elucidate the interactions of segmental peptides of α-synuclein with DPPC akyl chains

To do this, segmental peptides of α-syn were synthesized, purified, and studied at the air-water interface in the presence of dipalmitoyl phosphatidylcholine (DPPC). Then,

the conformation and orientation of the segment peptides was studied by pMAIRS. The first segment is α-syn(71-82) and second segment is α-syn(66-85) which is critical for aggregation as mentioned above. The third segment is α-syn(57-102) which is more soluble. It was found that α-syn(71-82) cannot form a stable Langmuir monolayer at the interface but interacts with DPPC very intensively. On the other hand, α-syn(66-85) and α-syn(57-102) were found to form monolayer even in the absence of DPPC. After DPPC was added, the monolayer of α-syn(66-85) and α-syn(57-102) is not miscellaneous with that of DPPC, which determined by pMAIRS.

CHAPTER 2

2.1 Materials

Fluorenylmethyloxycarbonylchloride (Fmoc)-L-Alanine (99.91%), N^{α}-Fmoc-N^{γ}-trityl-L-Asparagine (99.69%), N^{α}-Fmoc-N^{δ}-trityl-L-Glutamine (99.61%), Fmoc-L-Glutamic acid γ-*tert*-butyl ester hydrate (99.11%), Fmoc-Glycine (99.37%), Fmoc-L-Leucine (99.80%), N^{α}-Fmoc-N^{ε}-Boc-L-Lysine (99.84%), Fmoc-*O*-*tert*-butyl-L-Serine (99.83%), Fmoc-L-Valine (99.53%), and Wang Resin (0.3-0.8 meq/g, 200-400 mesh) (>99.00%) all came from Chem-Impex International Inc. (Wood Dale, Illinois). N^{α}-Fmoc-L-Aspartic acid α-*tert*-butyl ester (99.69%) and N^{α}-Fmoc-L-Isoleucine (>98.00%) were purchased from Novabiochem Inc. (Hohenbrunn, Germany). Fmoc-Phe-OH (>99.00%) came from BACHEM Inc. (Torrance, CA). Both Fmoc-Thr(tBu)-OH (99.60%) and HOBT hydrate (1-hydroxybenzoyltriazole hydrate) (>99.00%) were from Anaspec Inc. (Fremont, CA). DCM (Dichloromethane) (99.60%), Acetonitrile-HPLC grade (99.95%), DMF (N,N-dimethylformamide) (99.80%), Ethyl Ether Anhydrous (Diethyl ether) (99.90%), and Acetic Anhydride (99.80%) were purchased from Fisher Scientific (Fairlawn, NJ). Piperidine (99.00%) and Tris (Triisopropysilane) (98.00%) came from Sigma-Aldrich (St. Louis, MO). DIC (N,N'-Diisopropylcarbodiimide) (99.00%) and TFA(Trifluoroacetic acid) (99.00%) came from Alfa Aesar (Ward Hill, MA). The ultra-high purity Nitrogen gas (99.99%) came from NexAir in Memphis, TN. The dipalmitoyl phosphatidylcholine (DPPC) was purchased from Avanti Polar Lipds Inc. (Birmingham, AL).

2.2 Peptide Synthesis

Peptides studied in this thesis were synthesized using solid phase peptide synthesis (SPPS). A CEM discover bio manual microwave peptide synthesizer (Figure 2.1) was utilized with Wang resin as the solid support. During synthesis, Fmoc chemistry is used as a protective approach. Fmoc group protects the amino group of the amino acids by inhibiting solution coupling of dissolved amino acids. The target peptide is produced from C-terminus to N-terminus by repeating the sequence coupling-washing-deprotection-washing-cleavage. During the coupling stage, the peptide is built beginning with the activation and coupling of the carboxylic acid terminus of the Fmoc-amino acid. The coupling of the first amino acid entails coupling its C-terminus to 0.2 molar equivalents of Wang resin. HOBt is incorporated to prevent racemization, and DIC is added to activate the carboxylic group. The amine group on the solid phase's surface reacted with the activated carboxylic group to generate an amide bond as shown in Figure 2.2. The resin was then washed and the surface of the solid phase is cleaned with DMF.

During the deprotection stage as shown in Figure 2.3, the Fmoc was deprotected by the piperidine diluted in DMF at a volume-to-volume ratio of 20%. Piperidine undergoes a reaction in which it attaches itself to the Fmoc group that is protecting the amine. As a result of this action, the amine group that was before protected has become deprotected and is now prepared for the next coupling. After that, DMF is utilized severally to wash the resin to remove the remaining piperidine.

The coupling and deprotection process was repeated until the target peptide has been synthesized. After the completion of the target peptide chain, the peptide was capped by being subjected to a treatment with acetic anhydride and DCM. Then, the peptide was extracted from the Wang resin by suspending it in a 20mL solution containing volume ratios of 75: 22: 1.5: 1.5 volumes of TFA, DCM, triisopropylsilane, and H_2O, respectively. This process was repeated three times. In the course of this procedure, side chain protective groups like Boc were eliminated, which resulted in the synthesis of a linear crude peptide. H_2O and triisopropylsilane were utilized to prevent unwanted side reactions with reactive cationic species during side chain deprotection.

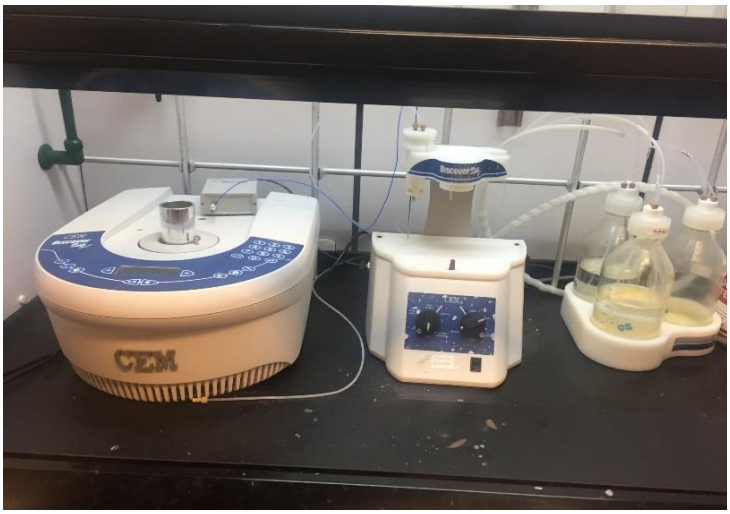

Figure 2.1: CEM Discover Bio Manual Microwave Peptide Synthesizer

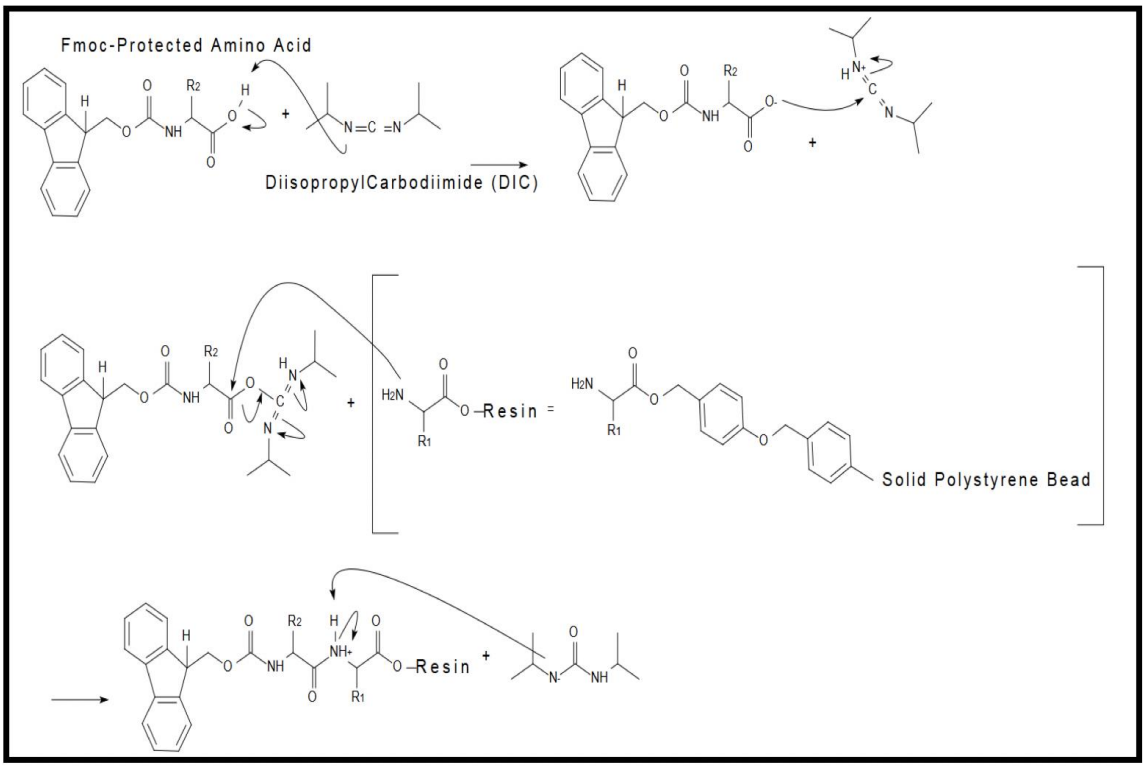

Figure 2.2 Coupling reaction during peptide synthesis

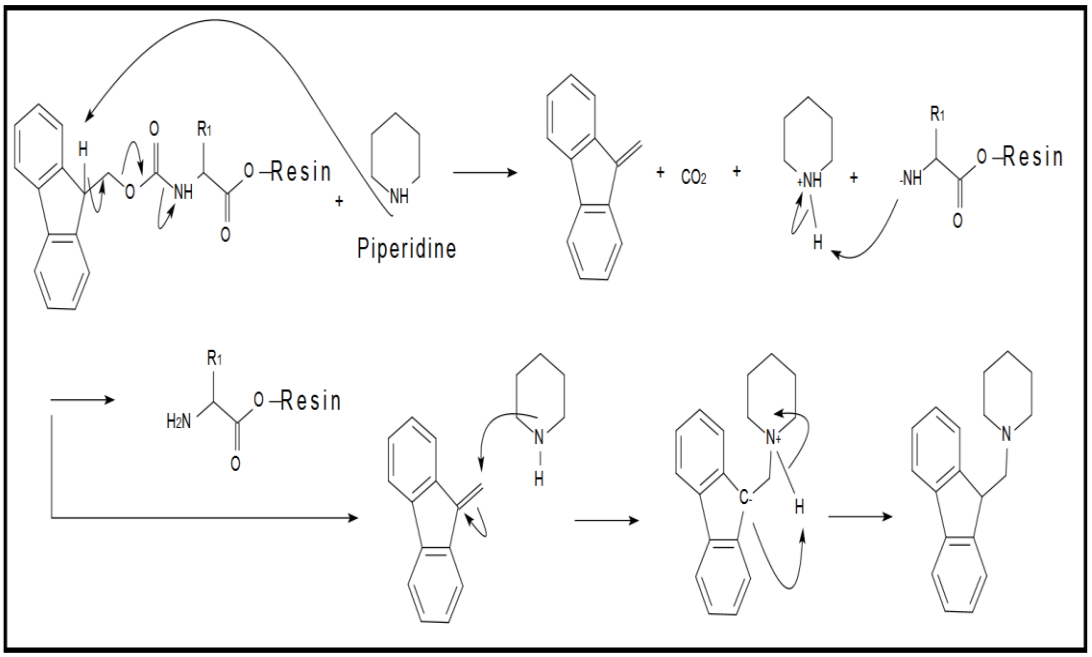

Figure 2.3 Deprotection reaction during peptide synthesis

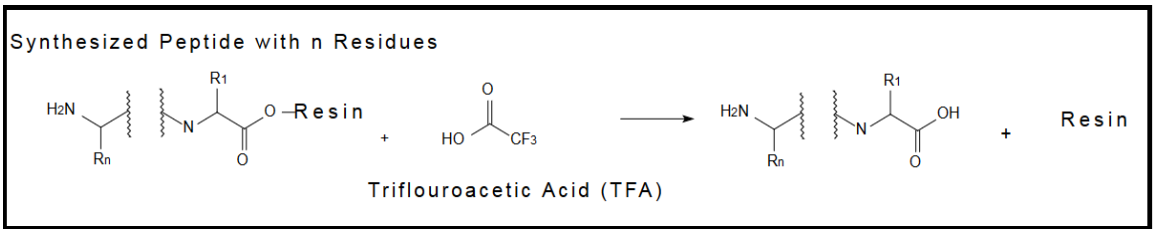

Figure 2.4 Cleavage reaction during peptide synthesis

2.3 High Pressure Liquid Chromatography (HPLC)

The process used to purify the proteins utilized in the studies is called high performance liquid chromatography (HPLC). A Waters 1525 Binary Solvent Pump connected to a Phenomenex Reverse Phase Semi Prep C18 Column, Jupiter Model 00G-4055-P0, with an internal diameter of 21.5 mm and a length of 250 mm was used to carry out the HPLC purification in this thesis. The Pump was connected to a Waters 2489 UV-Vis detector, which used a wavelength of 210 nm to detect UV absorption. Figure 2.5 displays the Waters 1525 Binary Solvent Pump and the Waters 2489 UV-Vis detector. The mobile phase B included HPLC grade acetonitrile and the mobile phase A contained a solution of 18.2 deionized water to 0.1 % TFA (v/v).

For the accurate separation of the pure peptide, a method development process was carried out for each peptide. A linear gradient of 25–80 percent by volume of A and B was used to purify peptide 71–82 during the course of 8 minutes at a flow rate of 21.2 mL/min. Using a linear gradient ratio of 34–39 percent by volume of A and B for 8 minutes at a flow rate of 21.2 mL/minute, peptide 66–85 was isolated. Finally, a linear gradient ratio of

30 to 100 percent by volume of A and B was used to purify peptide 57-102 over the course of 10 minutes at a flow rate of 10.0 mL/min. Each collected purified peptide was frozen at -80 °C before being lyophilized to produce the solid form of the purified peptides.

Figure 2.5 Waters 1525 Binary HPLC Pump with Waters 2489 UV/Visible Detector

2.4 Mass Spectroscopy

A great method for identifying a large range of chemical substances is mass spectroscopy (MS). It is employed to ascertain a particle's mass, a sample's elemental make-up, and the chemical structure of larger molecules. By using MS from a Waters SYNAPT q-TOF tandem mass spectrometer with electron spray ionization and an APCI

ion source (Figure 2.6), each peptide's successful synthesis and purification were verified. All the mass spectrometric measurements in this thesis were accomplished with this equipment, however the results was not included in this thesis write up because similar results have been previously reported in a publication by my research group. Before assessing the mass, each crude peptide was added to water and sonicated until dissolved. The sample was placed in a 100-L syringe. The capillary voltage was set to 3 keV, and the sample cone temperature for the MS was 150 °C. Nitrogen gas (N_2) was used at a rate of 500 L/h to evaporate the aqueous peptide solution containing 0.1% of TFA. The flow rate was set to 20, the run duration was set to 0.5 minutes, the scan time was set to 0.5 seconds, and the positive ion mode was used for the MS measurements.

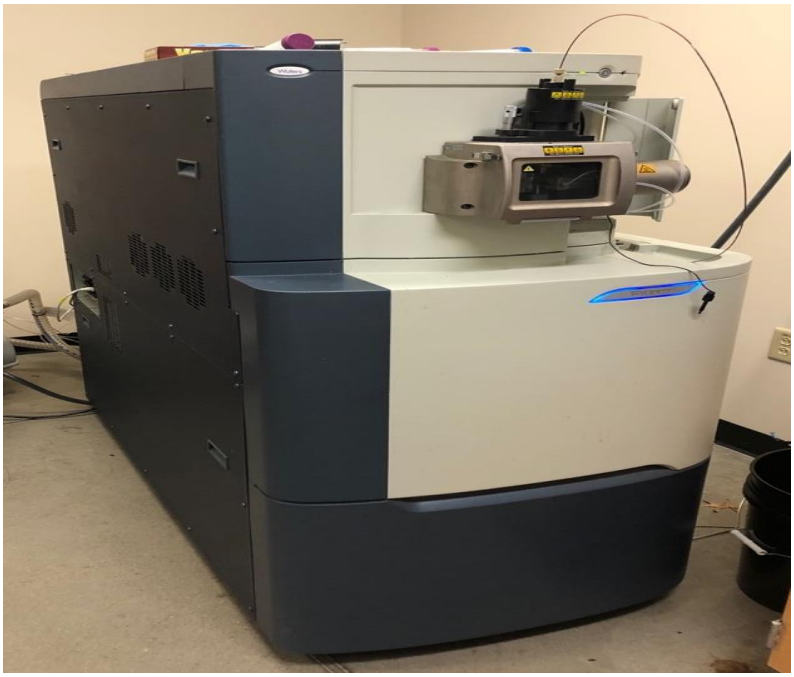

Figure 2.6 Waters synapt tandem mass spectrometer with time-of-flight configuration

2.5 Langmuir Monolayer Technique

A Kibron μtrough Langmuir trough XS (Kibron Inc., Helsinki Finland), as shown in Figure 2.7, was used for the study of the surface pressure-area (π-A) isotherms of dipalmitoyl phosphatidylcholine (DPPC) in the absence and presence of the various segment of α-synuclein. 20 mL DPPC solution with the concentration of 0.2 mg/mL in chloroform/methanol was spread at the interface. When in the presence of peptides, 0.1 mg/mL and 15 μL of the various segments of α-synuclein was also spread on air-water interface together with DPPC by a 25 μL syringe (Hamilton Inc., Reno, Nevada). When transferring the monolayer to quartz slide, the monolayer was held for two hours under the surface pressure of 10 mN/m and then, the quartz slide was moved slowly upward at 0.3 cm/minute.

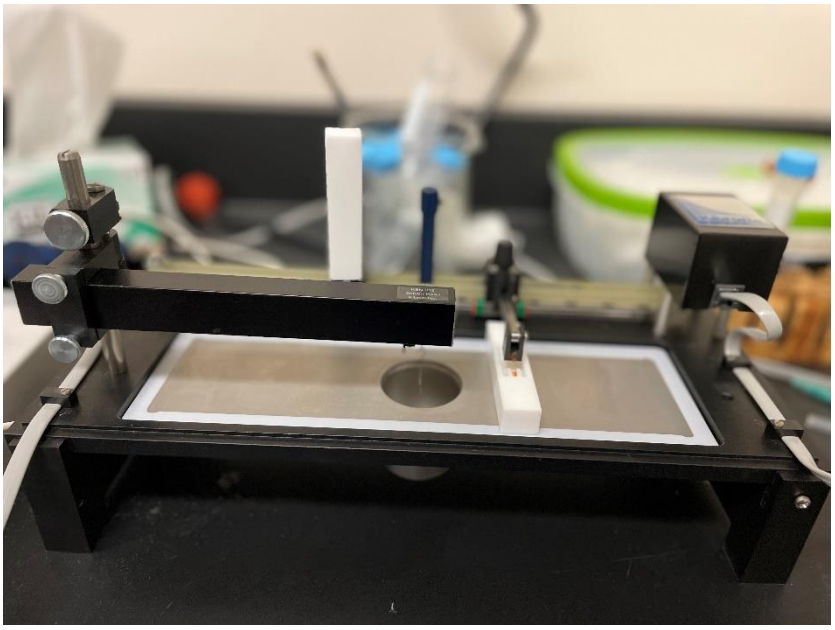

Figure 2.7 Langmuir trough

2.6 pMAIRS

pMAIRS measurements were performed on the Nicolet IS50 FTIR spectrometer (Thermo Scientific, Waltham, MA) equipped with a pMAIRS accessory as shown in Figure 2.8. The LB film monolayer on Si substrate was put in the pMAIRS accessory and the IR beam transmitted trough the sample. The refractive IR beam went to a HgCdTe (MCT) detector cooled by liquid nitrogen and the bare Si substrate was used as the background for measuring spectra of the sample monolayer. The spectra of both background and sample were acquired with a resolution of 8 cm^{-1} by an average of several thousand scans under the optimal conditions for a Si substrate. All the measurement were repeated three times at 9000 scans and the reported results in this thesis is the average of the three measurements

The in-plane (IP) and out-of-plane (OP) spectra were calculated by the p-MAIRS software according to all the background and sample results under various incident angles from 9º to 44º. It is worth noting that 44º is the maximum tilted angle of the slides and not that of the vibration-tilted angle.

The orientation/tilt angle (i.e., ϕ in equation 2.1 below) of a vibration to the surface normal was calculated the following equation:

$$\phi = \tan^{-1}\sqrt{\frac{2A_{IP}}{A_{OP}}} \qquad \text{Equation 2.1}$$

Figure 2.8 Thermo Fischer Nicolet iS50R FTIR

Chapter 3

Results and Discussion

3.1 Interaction of DPPC with NAC Segment Peptides

The interaction of DPPC with the NAC segment peptides was studied by the Langmuir monolayer technique and the surface pressure-area (π—A) isotherms are shown below. Figure 3.1 shows the π—A isotherm of DPPC in the absence of any peptides. The take-of point of the π—A isotherm was at 65 $Å^2$/molecule and then the surface pressure increases slowly up to twist point at 42 $Å^2$/molecule. When the surface area is further decreased, a quick increase in the surface pressure occurs and a fall was observed at surface pressure 50 mN/m with 25 $Å^2$/molecule. This result is similar to the published one whereas the addition of peptides changed isotherm substantially.

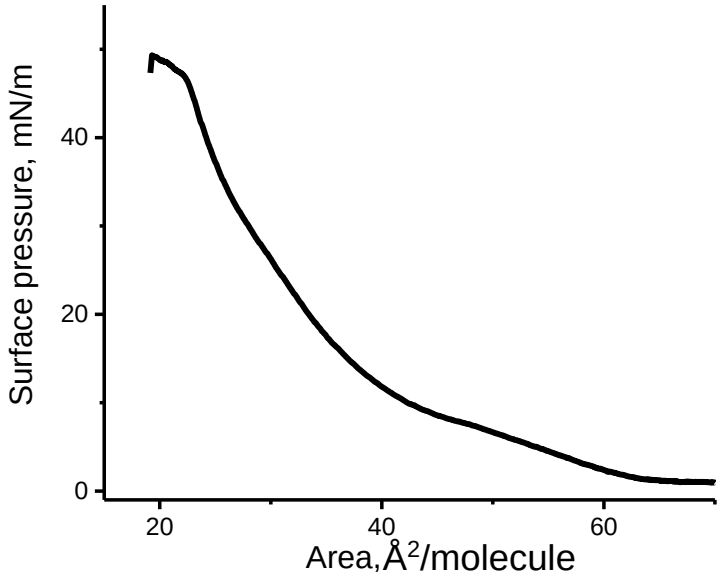

Figure 3.1 The surface pressure-area (π—A) isotherm of DPPC only.

Figure 3.2 shows the π－A isotherm of DPPC in the presence of α-syn(61-95). The isotherm shows a lift-off point around 360 $Å^2$/molecule and the twist point increases to 105 $Å^2$/molecule compared with the isotherm of DPPC only in Figure 3.1. After that, surface pressure also increases sharply until the monolayer collapses around 90 $Å^2$/molecule with surface pressure around 50 mN/m. The π－A isotherms of DPPC in the presence of α-syn(66-85) and α-syn(57-102) are shown in Figure 3.3 and 3.4, respectively. Both of the isotherms are similar to that shown in Figure 3.2. However, the isotherm of DPPC in the presence α-syn(71-82) is different.

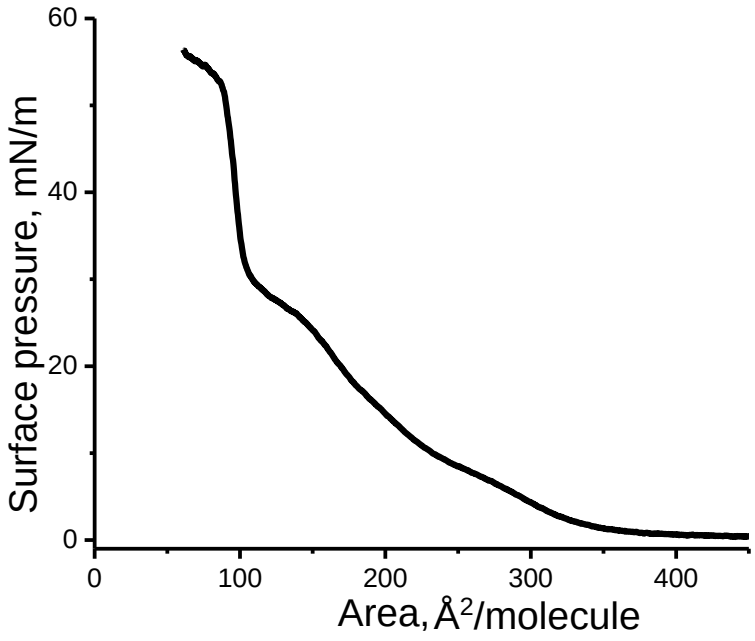

Figure 3.2 The π－A isotherm of DPPC in the presence of α-syn(61-95) in the subphase.

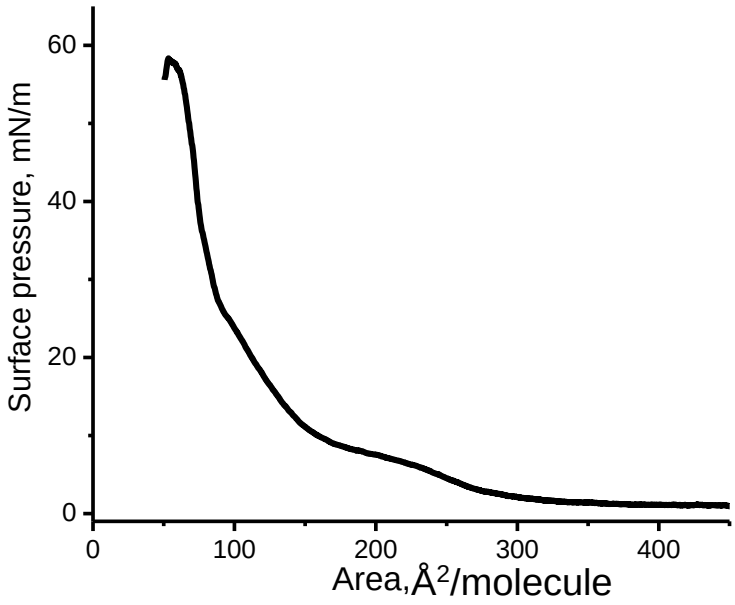

Figure 3.3 The π－A isotherm of DPPC in the presence of α-syn(66-85) in the subphase.

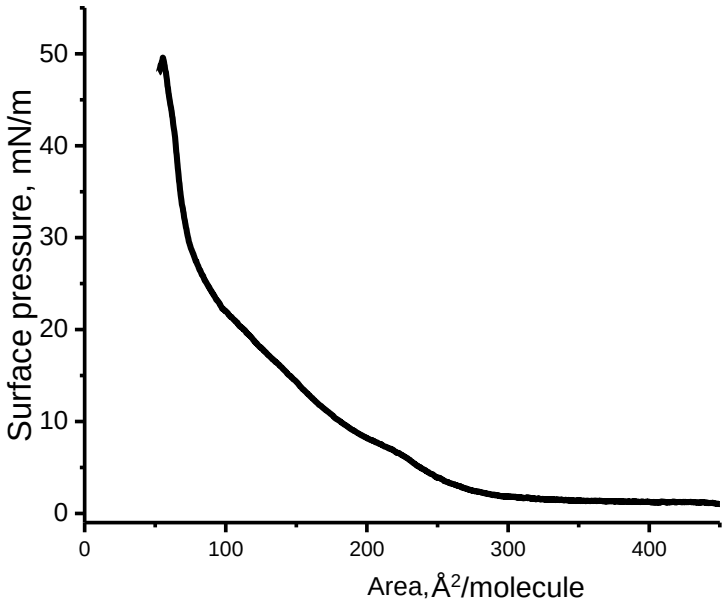

Figure 3.4 The π－A isotherm of DPPC in the presence of α-syn(57-102) in the subphase.

Different to the isotherms mentioned above, the π－A isotherm of DPPC in the presence of α-syn(71-82) exhibits a much bigger lift-off point around 2300 Å^2/molecule

as shown in Figure 3.5. The twist point increases to 1000 $Å^2$/molecule and surface pressure increases quickly after it. The isotherm collapses around 550 $Å^2$/molecule with surface pressure at 53 mN/m. To investigate the reason of this substantial difference, pMAIRS was employed to study the structure of the monolayer.

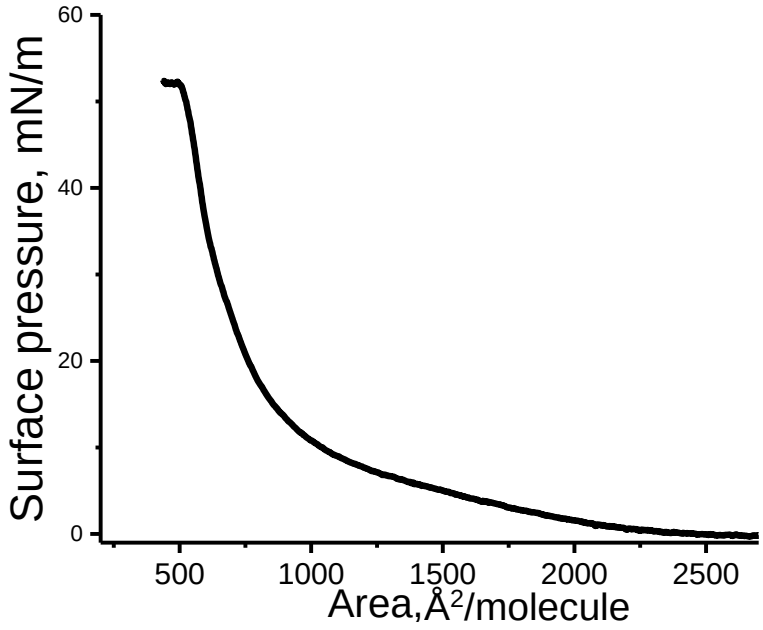

Figure 3.5 The π—A isotherm of DPPC in the presence of α-syn(71-82) in the subphase.

3.2 pMAIRS Results of DPPC Monolayer with NAC Segment Peptides

Figure 3.6 depicts the pMAIRS results of DPPC monolayer in the absence of peptide.The stretching mode of CH_2 of the alkyl chains in DPPC was clearly detected at 2918 and 2848 cm^{-1} in the in-plane spectrum (S_{IP}) even in monolayer structure. The stretching mode of carbonyl (i.e., C=O) in DPPC was also detected at 1730 cm^{-1} in the S_{IP}. Due to the extremely low thickness of the monolayer, other peaks are not with good

signal-to-noise ratio. As for the out-of-plane spectrum (S_{OP}), the carbonyl peak at 1730 cm^{-1} is not with good-to-noise signal ratio. According to the selection rules of pMAIRS as discussed in Chapter 1, a strong peak in S_{IP} whereas a weaker peak in S_{OP} means the vibration is parallel to the surface. Therefore, the carbonyl is roughly parallel to the surface, although the tilted angle cannot be accurately evaluated due to the low signal-to-noise ratio in S_{OP}. Interestingly, the peak of CH_2 at 2918 and 2848 cm^{-1} is also strong in S_{IP} but weaker in S_{OP}. Different to carbonyl, the peak of CH_2 in S_{OP} is still with good signal-to-noise ratio. Thus, the tilted angle of CH_2 is 79 $^{o}\pm1^{o}$. After α-syn(61-95) was added to the subphase, the pMAIRS results of DPPC with α-syn(61-95) is shown in Figure 3.7. Although the peptide is in the subphase, the amide bands was not clearly detected which may be because the transference of peptides to the interface is not high enough to provide a signal.

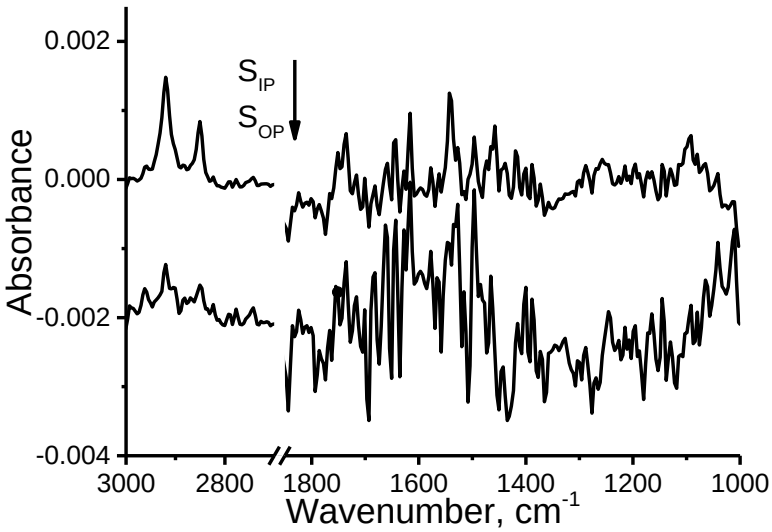

Figure 3.6 The pMAIRS results of DPPC only in monolayer.

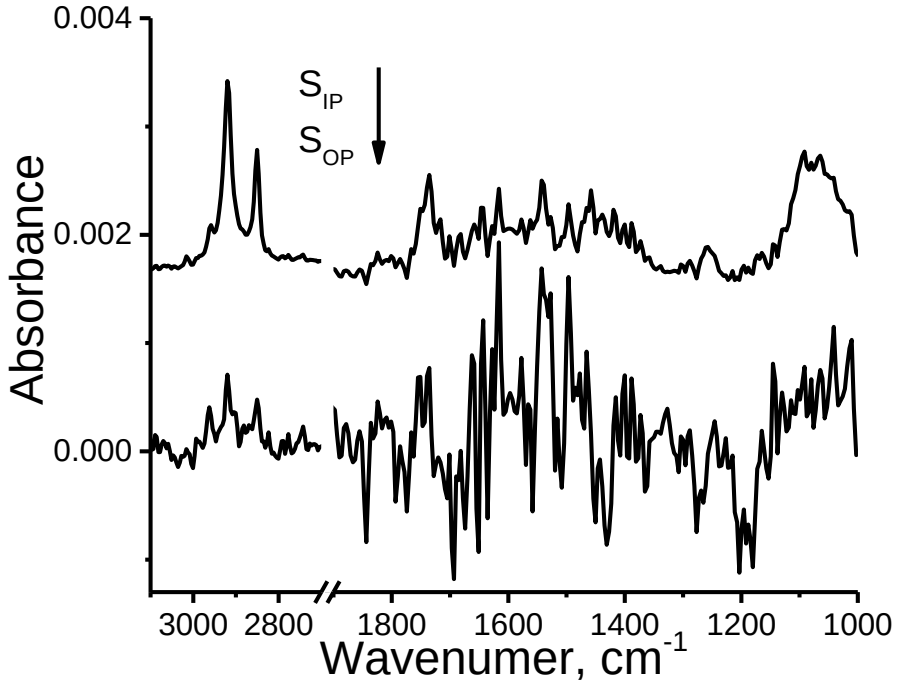

Figure 3.7 The pMAIRS results of DPPC with α-syn(61-95) in monolayer.

The tilted angle of CH_2 in Figure 3.7 is similar to that of Figure 3.6. This indicates the interaction of DPPC with α-syn(61-95) is not strong enough and the DPPC may not be miscellaneous with α-syn(61-95) in the monolayer. Similar results were also detected in the monolayer of DPPC with α-syn(66-85) and α-syn(57-102), as the pMAIRS results shown in Figure 3.8 and 3.9, respectively. However, as its π—A isotherm is different to others as shown abolve, the pMAIRS results of DPPC with α-syn(71-82) are also different to the others as shown in Figure 3.10.

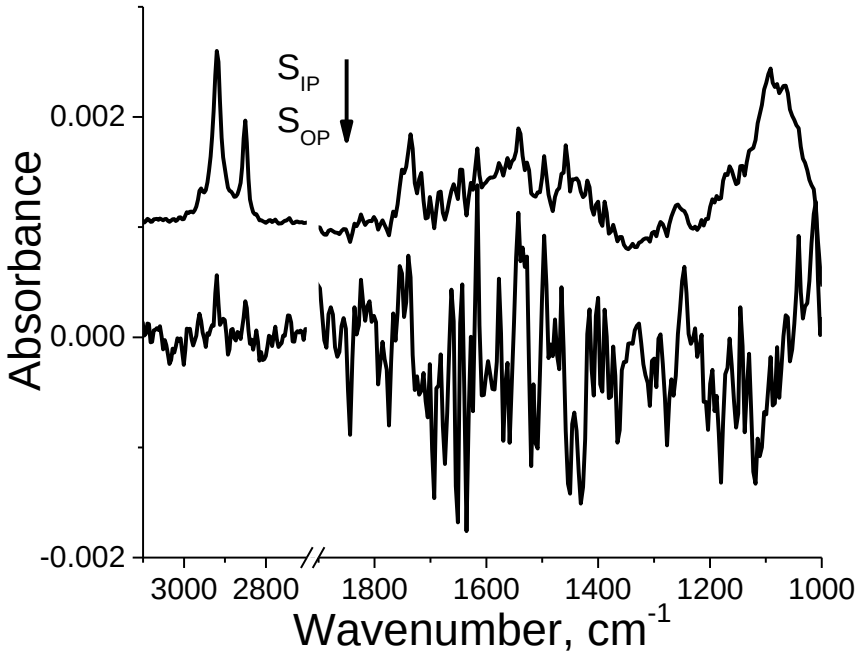

Figure 3.8 The pMAIRS results of DPPC with α-syn(66-85) in monolayer.

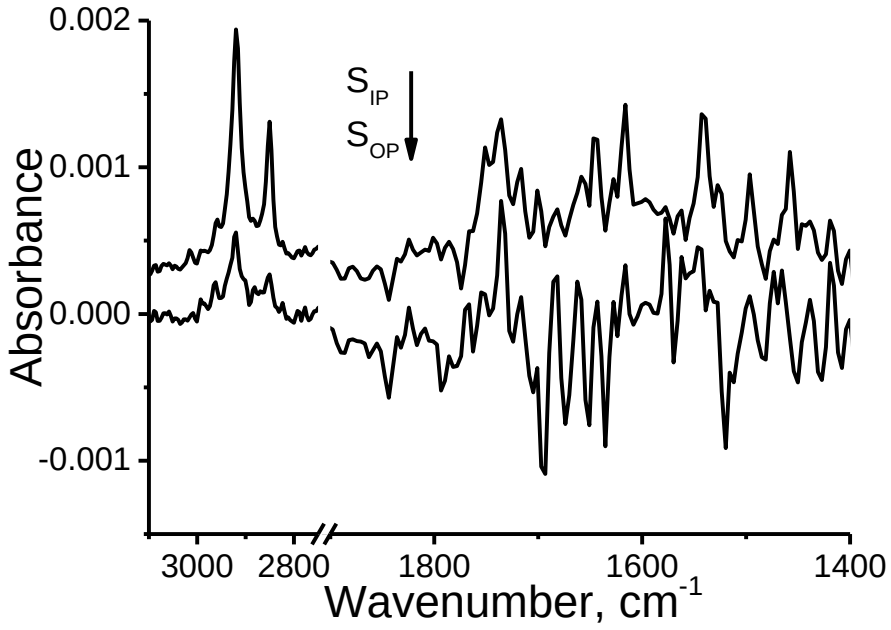

Figure 3.9 The pMAIRS results of DPPC with α-syn(57-102) in monolayer.

In Figure 3.10, the amide as well as the carbonyl bands between 1900 and 1400 cm^{-1} are not with good signal-to-noise, either. The major difference in Figure 3.10 stems from the peak intensity of CH_2 at 2918 and 2848 cm^{-1}. Besides the clear peaks of CH_2 in S_{IP}, these peaks are also with good signal-to-noise ratio in S_{OP} with stronger peak intensity than other peptides with DPPC. The tilted angle of the alkyl chains of DPPC calculated by the peak intensity of CH_2 in Figure 3.10 is 76 °±1°.

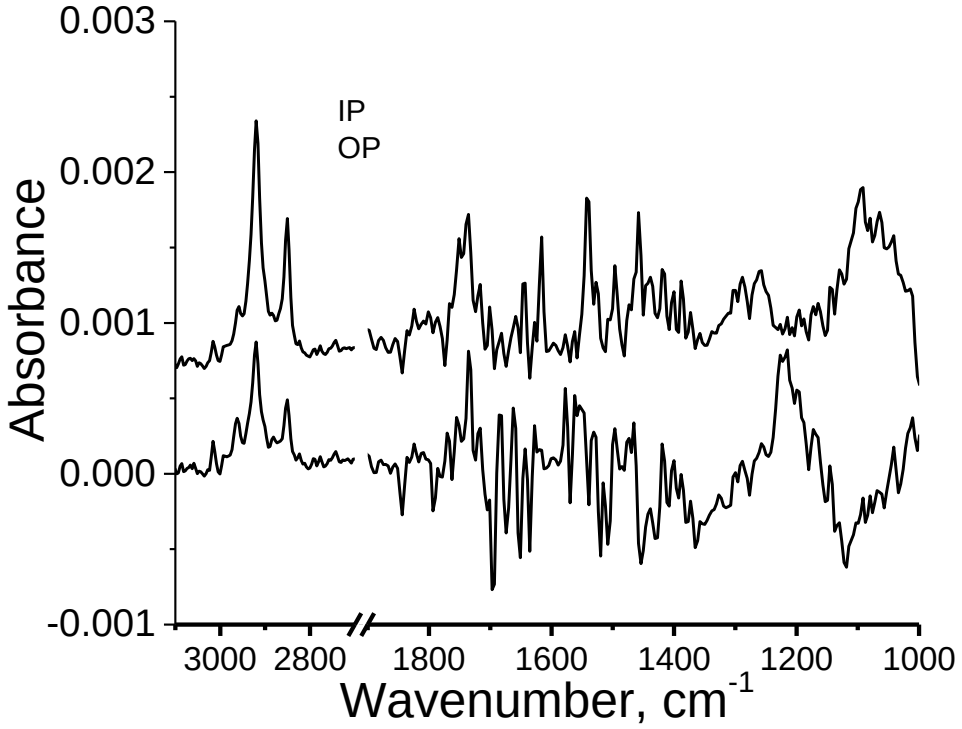

Figure 3.10 The pMAIRS results of DPPC with α-syn(71-82) in monolayer.

Chapter 4

Conclusion and Future Plan

In general, α-syn(66-85), α-syn(61-95), and α-syn(57-102) can form a stable monolayer at the air-water interface. The monoalyer formed by the segment peptides mentioned above does not interact with DPPC. This indicates that the lipid-water interfacial layer around phospholipids affects the biophysical behavior of the segment peptides above, whereas the other two layer (i.e., the hydrophobic layer comprising alkyl chains and the hydrophilic headgroups) of phospholipids do not affect as shown in Scheme 3.1A below. On the contrary, α-syn(71-82) cannot form a monolayer by itself at the air-water interface but can interact with DPPC intensively. α-Syn(71-82) is supposed to insert between the DPPC molecules in the monolayer as shown in Schme 3.1B, because the tilted angle of the alkyl chain decreased in the presence of α-syn(71-82) according to the pMAIRS results shown in Figure 3.10. Why does this happen? As discussed in **Chapter 1**, the intermolecular interaction between peptides depends on the size of molecule. A longer sequence of peptide may intensify the interaction between the peptides and therefore, peptides will aggregate together and may not be miscellenous with lipid molecule. Further investigation is needed to prove this hypothesis.

Scheme 3.1 The interaction between DPPC and α-syn segment peptides.

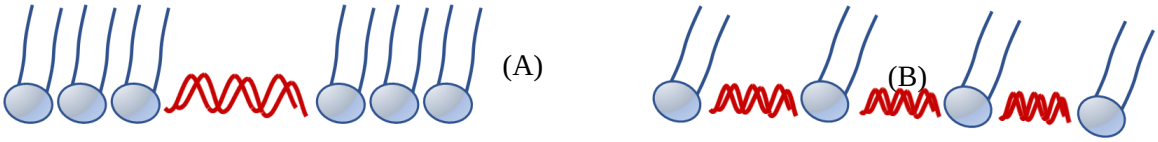

On the other hand, the signal-to-noise ratio of amide I and amide II bands is not very good. Consequently, several very important questions cannot be addressed as following. First, what is the conformation of the segmental peptides in the presence of DPPC? It is more probable that α-syn(66-85), α-syn(61-95), and α-syn(57-102) are still in α-helix as they form stable monolayer by themselves, especially when the peptide monolayer is not be miscellenous with DPPC. However, the conformation of α-syn(71-82) needs to be determined and this was not accomplished here. Second, what is the tilted angle of the axis of α-helix of the segmental peptides? Again, it is probable that the tilted angle of α-syn(66-85), α-syn(61-95), and α-syn(57-102) are still the same as they form stable monolayer by themselves. Whereas the tilted angle of α-syn(71-82) also needs to be evaluated. How to improve the signal-to-noise ratio then? There are several future plans. First, the sensitivity of the MCT detector keeps improving in the last two decades. For example, Thermo-Fisher offered MCT-B detector around 2010 and provided a more powerful MCT-D* dector recently. We believe that a more sensitive detector will be available soon. Second, the container of liquid N_2 of the MCT detector also keeps increasing. A bigger container of liquid N_2 will allow longer measurements and more scans, which will also increase the signal-to-noise ratio. We will keep our attention on the update of new parts of FT-IR spectrometer and hope to resolve this problem as soon as we can.

References

1. Giasson, B. I.; Murray, I. V. J.; Trojanowski, J. Q.; Lee, V. M. Y., A hydrophobic stretch of 12 amino acid residues in the middle of a-synuclein is essential for filament assembly. *J. Biol. Chem.* **2001,** *276*, 2380-2386.

2. Efimova, Y. M.; Haemers, S.; Wierczinski, B.; Norde, W.; van Well, A. A., Stability of globular proteins in H_2O and D_2O. *Biopolymers* **2007,** *85*, 264-273.

3. Fabre, R. M.; Okeyo, G. O.; Talham, D. R., Supported lipid bilayers at skeletonized surfaces for the study of transmembrane proteins. *Langmuir* **2012,** *28*, 2835-2841.

4. Keaney, J. F.; Frei, B., *Antioxidant protection of low-density lipoprotein and its role in the prevention of atherosclerotic vascular disease*. Academic Press: San Diego, 1994; p 303-352.

5. Mattson, M. P., *Protein Phosphorylation in Aging and Age-Related Disease (Advances in Cell Aging and Gerontology Series, 16)* 1ed.; Elsevier Publishing Company: 2004.

6. Varadarajan, S.; Yatin, S.; Aksenova, M.; Butterfield, D. A., Review: Alzheimer's amyloid b-peptide-associated free radical oxidative stress and neurotoxicity. *J. Struct. Biol.* **2000,** *130*, 184-208.

7. Wevers, R. A.; de Rijk-van Andel, J. F.; Brautigam, C.; Geurtz, B.; van den Heuvel, L.; Steenbergen-Spanjers, G. C. H.; Smeitink, J. A. M.; Hoffmann, G. F.; Gabreels, F. J. M., A review of biochemical and molecular genetic aspects of tyrosine hydroxylase deficiency including a novel mutation (291delC). *J. Inherited Metabolic Dis.* **1999**, 364-373.

8. Kahn, R.; Carpentier, P.; Berthet-Colominas, C.; Capitan, M.; Chesne, M. L.; Fanchon, E.; Lequien, S.; Thiaudiere, D.; Vicat, J.; Zielinski, P.; Stuhrmann, H., Feasibility and review of anomalous X-ray diffraction at long wavelengths in materials research and protein crystallography. *J. Synchrotron Radiat.* **2000,** *7*, 131-138.

9. Madine, J.; Doig, A. J.; Middleton, D. A., Design of N-methylated peptide inhibitor of a-synuclein aggregation guided by solid-state NMR. *J. Am. Chem. Soc.* **2008,** *130*, 7873-7881.

10. Nair, N. G.; Perry, G.; Smith, M. A.; Reddy, V. P., NMR studies of zinc, copper, and iron binding to histidine, the principal metal ion complexing site of amyloid-β peptide. *J. Alzheimer's Dis.* **2010,** *20*, 57-66.

11. Orcellet, M. L.; Fernandez, C. O., Structures behind the amyloid aggregation of a-synuclein: An NMR based approach. *Current Protein Peptide Sci.* **2011,** *12*, 188-205.

12. Combs, J. D.; Gonzalez, C. U.; Wang, C., Surface FTIR techniques to analyze the conformation of proteins/peptides in H_2O environment. *J. Phys. Chem. Biophys.* **2016,** *6*, 1.

13. Spillantini, M. G.; Crowther, R. A.; Jakes, R.; Hasegawa, M.; Goedert, M., a-Synuclein in filamentous inclusions of Lewy bodies from Parkinson's disease and dementia with Lewy bodies. *Proc. Natl. Acad. Sci. U. S. A.* **1998,** *95*, 6469-6473.

14. Spillantini, M. G.; Schmidt, M. L.; Lee, V. M. Y.; Trojanowski, J. Q.; Jakes, R.; Goedert, M., a-Synuclein in Lewy bodies. *Nature* **1997,** *388*, 839-840.

15. Fink, A. L., The aggregation and fibrillation of a-synuclein. *Acc. Chem. Res.* **2006,** *39*, 628-634.

16. Qin, Z.; Hu, D.; Han, S.; Hong, D.; Fink, A. L., Role of different regions of a-synuclein in the assembly of fibrils. *Biochemistry* **2007,** *46*, 13322-13330.

17. Wright, J. A.; Brown, D. R., Alpha-synuclein and its role in metal binding: Relevance to Parkinson's disease. *J. Neurosci. Res.* **2008,** *86*, 496-503.

18. Breydo, L.; Wu, J. W.; Uversky, V. N., Alpha-synuclein misfolding and Parkinson's disease. *Biochim. Biophys. Acta.* **2012,** *1822*, 261-285.

19. Han, H.; Weinreb, P. H.; Lansbury, P. T., The core Alzheimer's peptide NAC forms amyloid fibrils which seed and are seeded by beta-amy loid: Is NAC a common trigger or target in neurodegenerative disease? *Chem. Biol.* **1995,** *2*, 163-169.

20. Massover, W. H., Radiation damage to protein specimens from electron beam imaging and diffraction: a mini-review of anti-damage approaches, with special reference to synchrotron X-ray crystallography. *J. Synchrotron Radiat.* **2007,** *14*, 116-127.

21. Celej, M. S.; Sarroukh, R.; Goormaghtigh, E.; Fidelio, G. D.; Ruysschaert, J. M.; Raussens, V., Toxic prefibrillar a-synuclein amyloid oligomers adopt a distinctive antiparallel b-sheet structure. *Biochem. J.* **2012,** *443*, 719-726.

22. Krogh, A.; Larsson, B.; Heijne, G.; Sonnhammer, E. L. L., Predicting transmembrane protein topology with a hidden Markov model: Application to complete genomes. *J. Struct. Biol.* **2001,** *305*, 567-580.

23. Manor, J.; Arbely, E.; Beerlink, A.; Akkawi, M.; Arkin, I. T., Use of isotope-edited FTIR to derive a backbone structure of a transmembrane protein. *J. PHys. Chem. Lett.* **2014,** *5*, 2573-2579.

24. Heise, H.; Hoyer, W.; Becker, S.; Andronesi, O. C.; Riedel, D.; Baldus, M., Molecular-level secondary structure, polymorphism, and dynamics of full-length alpha-

synuclein fibrils studied by solid-state NMR. *Proc. Nat. Acad. Sci. U.S.A.* **2005,** *102* (15871-15876).

25. Vilar, M.; Chou, H. T.; Lührs, T.; Maji, S. K.; Riek-Loher, D.; Verel, R. M., G.; Stahlberg, H.; Riek, R., The fold of a-synuclein fibrils. *Proc. Nat. Acad. Sci. U.S.A.* **2008,** *105*, 8637-8642.

26. Gaggelli, E.; Kozlowski, H.; Valensin, D.; Valensin, G., Copper homeostasis and neurodegenerative disorders (Alzheimer's, prion, and Parkinson's diseases and amyotrophic lateral sclerosis). *Chem. Rev.* **2006,** *106*, 1995-2044.

27. Scheidt, H. A.; Morgado, I.; Rothemund, S.; Huster, D., Dynamics of amyloid-b fibrils revealed by solid-state NMR. *J. Biol. Chem.* **2012,** *287*, 2017-2021.

28. Sreerama, N.; Woody, R. W., Estimation of protein secondary structure from CD spectra: Comparison of CONTIN, SELCON and CDSSTR methods with an expanded reference set. *Anal. Biochem.* **2000,** *282*, 252-260.

29. Dziri, L.; Desbat, B.; Leblanc, R. M., Polarization modulated FT-IR spectroscopy studies of acetylcholinesterase secondary structure at the air-water interface. *J. Am. Chem. Soc.* **1999,** *121*, 9618-9625.

30. Yang, G.; Dong, Y.; Gong, K.; Jiang, W.; Kwon, E.; Wang, P.; Zheng, H.; Zhang, X.; Gan, W.; Zhao, N., Reduced synaptic vesicle density and active zone size in mice lacking amyloid precursor protein (APP) and APP-like protein 2. *Neurosci. Lett.* **2005,** *384*, 66-71.

31. Fabre, R. M.; Talham, D. R., Stable supported lipid bilayers on zirconium phosphonate surfaces. *Langmuir* **2009,** *25*, 12644-12652.

32. Du, X.; Miao, W.; Liang, Y., IRRAS studies on chain orientation in the monolayers of amino acid amphiphiles at the air-water interface depending on metal complex and hydrogen bond formation with the headgroups. *J. Phys. Chem. B* **2005,** *109*, 7428-7434.

33. Hasegawa, T.; Nishijo, J.; Watanabe, M.; Umemura, J.; Ma, Y.; Sui, G.; Huo, Q.; Leblanc, R. M., Characteristics of long-chain fatty acid monolayers studied by infrared external-reflection spectroscopy. *Langmuir* **2002,** (12), 4758-4764.

34. Wang, C.; Micic, M.; Ensor, M.; Daunert, S.; Leblanc, R. M., Infrared reflection-absorption spectroscopy and polarization-modulated infrared reflection-absorption spectroscopy studies of the aequorin Langmuir monolayer. *J. Phys. Chem. B* **2008,** *112*, 4146-4151.

35. Wang, C.; Shah, N.; Thakur, G.; Zhou, F.; Leblanc, R. M., a-Synuclein in a-helical conformation at the air-water interface: Implication of conformation and orientation changes during its accumulation/aggregation. *Chem. Commun.* **2010,** *46*, 6702-6704.

36. Wang, C.; Zheng, J.; Zhao, L.; Rastogi, V. K.; Shah, S. S.; DeFrank, J. J.; Leblanc, R. M., Infrared reflection-absorption spectroscopy and polarization-modulated Infrared Reflection-Absorption Spectroscopy studies of the organophosphorus acid anhydrolase Langmuir monolayer. *J. Phys. Chem. B* **2008,** *112*, 5250-5256.

37. Hasegawa, T., *Quantitative Infrared spectroscopy for understanding of a condensed matter*. Springer 2017; p 1-193.

38. Wang, C.; Sharma, S. K.; Olaluwoye, S. O.; Alrashdi, S. A.; Hasegawa, T.; Leblanc, R. M., Conformation change of α-synuclein(61－95) at the air-water interface

and quantitative measurement of the tilt angle of the axis of its α-helix by multiple angle incidence resolution spectroscopy. *Colloid. Surf. B* **2019,** *183*, 110401.

39. Decatur, S. M., Elucidation of residue-level structure and dynamics of polypeptides via isotopp-edited infrared spectroscopy. *Acc. Chem. Res.* **2006,** *39*, 169-175.

40. Beyer, K., a-Synuclein structure, posttranslational modification and alternative splicing as aggregation enhancers. *Acta Neuropathol.* **2006,** *112*, 237–251.

41. Borbat, P.; Ramlall, T. F.; Freed, J. H.; Eliezer, D., Inter-helix distances in lysophospholipid micelle-bound a-synuclein from pulsed ESR measurements. *J. Am. Chem. Soc.* **2006,** *128*, 10004-10005.

42. Kamp, F.; Beyer, K., Binding of a-synuclein affects the lipid packing in bilayers of small vesicles. *J. Biol. Chem.* **2006,** *281*, 9251-9259.

43. Stockl, M.; Fischer, P.; Wanker, E.; Herrmann, A., α-Synuclein selectively binds to anionic phospholipids embedded in liquid-disordered domains. *J. Mol. Biol.* **2008,** *375*, 1394-1404.

44. Munishkina, L. A.; Phelan, C.; Uversky, V. N.; Fink, A. L., Conformational behavior and aggregation of a-synuclein in organic solvents: Modeling the effects of membranes. *Biochemistry* **2003,** *42*, 2720-2730.

45. Teschke, O.; de Souza, E. F., Liposome structure imaging by atomic force microscopy: Verification of improved liposome stability during adsorption of multiple aggregated vesicles. *Langmuir* **2002,** *18*, 6513-6520.

46. Teschke, O.; de Souza, E. F., Water molecular arrangement at air/water interfaces probed by atomic force microscopy. *Chem. Phys. Lett.* **2005,** *403*, 95-101.

47. Miles A J, Wallace B A. Biopharmaceutical applications of protein characterisation by circular dichroism spectroscopy//Biophysical Characterization of Proteins in Developing Biopharmaceuticals. Elsevier, 2020: 123-152.